



# Treatment of high-phosphorus load wastewater by column packed with non-burning compound filler/gravel/ceramsite: evaluation of performance and microorganism community

Qiang Li<sup>1,2</sup> · Jingqing Gao<sup>1,3</sup> · Jingshen Zhang<sup>2</sup> · Zhenzhen Huang<sup>1,4</sup> · Shilong Wang<sup>1</sup> · Bozhen Song<sup>1</sup> · Qiaojian Wang<sup>1</sup> · Wanglin Zhou<sup>5</sup>

Received: 17 July 2022 / Accepted: 13 March 2023 / Published online: 28 April 2023  
© The Author(s), under exclusive licence to Springer-Verlag GmbH Germany, part of Springer Nature 2023

## Abstract

Cost-effective and environmental-friendly substrates are essential for the constructed wetlands (CWs). In this study, the column test was used to explore the differences in pollutant purification performance, microbial community structure and abundance between non-burning compound filler and conventional CWs substrates (i.e. gravel and ceramsite) at low temperature (0–15°C). It was found that the maximum phosphorus removal efficiency of compound filler (99%) was better than gravel (18%) and ceramsite (21%). Besides, the proportion of aerobic heterotrophic bacteria capable of ammonium oxidation, nitrification and denitrification (i.e. *Pseudomonas*, *Acinetobacter*, and *Acetoanaerobium*) was enhanced by compound filler, which has an excellent potential for nitrogen removal in the subsequent purification process. These results demonstrated that the self-made non-burning compound filler was a potential substrate for CWs, which was of great significance for the resource utilization of solid wastes such as polyaluminum chloride residue.

**Keywords** Non-burning compound filler · Column experiments · Microbial community · Waste resource utilization · Constructed wetlands

---

Responsible Editor: Alexandros Stefanakis

✉ Jingqing Gao  
jingqinggao@zzu.edu.cn

<sup>1</sup> School of Ecology and Environment, Zhengzhou University, Zhengzhou 450001, China

<sup>2</sup> College of Chemistry, Zhengzhou University, Zhengzhou 450001, China

<sup>3</sup> Key Laboratory of Water Management and Water Security for Yellow River, Basin, Ministry of Water Resources (Under Construction), Zhengzhou 450001, China

<sup>4</sup> Faculty of Environmental and Municipal Engineering, Henan Province Key Laboratory of Water Pollution Control and Rehabilitation Technology, Henan University of Urban Construction, Pingdingshan 467036, China

<sup>5</sup> CSCEC Xinjiang Construction&Engineering (Group) Co.,Ltd, Xian 710000, China

## Introduction

With the increasing world population, excessive emissions of different pollutants (i.e. swine wastewater), has led to eutrophication of water bodies, namely the formation of detrimental algal blooms and the deterioration of water, which has become a global environmental problem that has aroused serious concern (Chang et al. 2019; Wang et al. 2018). Generally, high-load sewage contains organic compounds, ammonia nitrogen, phosphorus and so on, which can cause serious harm to the surface runoff (Scholes et al. 2008; Lu et al. 2021). Thus, remediation of high-load wastewater through the removal of nutrients such as nitrogen and phosphorus has become an urgent need for water body protection, and increasingly attention worldwide (Chang et al. 2019; Sheng et al. 2013).

In a variety of methods of purification, constructed wetlands (CWs) are promising and practical because they are less energy consumption, low investment, environment-friendly and operation-flexibly (Xiao et al. 2020; Wu et al. 2015). It is considered to be a multi mechanism processes for the removal of contaminants involving substrate

adsorption and precipitation, plant uptake and microbial degradation (Cheng et al. 2018). The substrates are the key factor in the purification process and the main components of CWs (Yang et al. 2018), especially in the northern part of China in winter low temperature season (0–15°C). Thus, the selection of substrate is one of the important technical problems in the application of CWs, and it is a challenge and research point.

Conventional substrates, such as gravel, soil and sand, are inefficient at removing contaminants (Brix et al. 2001; Yang et al. 2018). In recent years, ceramsite, zeolite, lava rock and other new functional porous materials have been widely used in CWs (Chang et al. 2019). Polyaluminum chloride residue (PACR) is unavoidable industrial by-products and general solid wastes in the field of water purification. At least 60 kt PACR is produced annually by polyaluminum chloride production enterprises in China, and direct dumping, landfill and incineration have serious harm environmental hazards. In our previous study, a new non-burning PACR compound filler was successfully prepared by our team based on the non-burning technology, and conducted a series of batch experiments studies on their properties and mechanisms, which is of great significance for the resource utilization of PACR (Li et al. 2021b; Gao et al. 2020).

However, batch experiments are simplicity and short time requirements to compare removal efficiency of different materials, the parameters of batch experiments are set arbitrarily, and the results are often non-comparable (Habibi-andehkordi et al. 2014; Blanco et al. 2016). Besides, the use of isotherm equations to estimate adsorption capacity of different materials in field-scale experiments may lead to biased and unrealistic. As a result, many scientists have carried out long-term column experiments, with the same factors such as hydraulic conditions of the simulation in CWs, the longevity and retention capacity of substrate to be estimated in CWs (Blanco et al. 2016).

In this study, three columns packed with non-burning PACR compound filler, gravel and clay ceramsite were established for the purification of high-phosphorus load wastewater under a continuous flow mode, and the purification performance and microorganism communities in the columns were studied. Thus, the specific objectives of this paper were: (1) compared the effect of PACR compound filler and other conventional substrates (such as gravel and ceramsite) on the pollutant removal in column experiments; (2) investigated the impact of the substrates (i.e. PACR compound filler, gravel and ceramsite) on the structure, diversity, and abundance of microorganism communities attached to the solid by high throughput sequencing; (3) evaluated the feasibility of PACR compound filler as the substrate of CWs, and provided theoretical basis and reference data for its large-scale application in the actual engineering of CWs in low temperature season.

## Materials and methods

### Physicochemical properties

Three substrates, i.e., PACR compound filler, gravel and ceramsite, were investigated in this study. Gravel and ceramsite were purchased from Henan Tongde Environmental Engineering Co., Ltd (Zhengzhou, Henan, China). The non-burning PACR compound filler were prepared according to the literature (Li et al. 2021b; Gao et al. 2020). PACR compound filler was prepared by non-burning consolidation technology. The optimal formula of PACR compound filler was determined by single factor and mixing design response optimization experiment as follows: cement 44%, PACR 49%, bentonite 7%. Three ingredients were mixed in the specified ratio, and the amount of water was added (mixture/water: 3/1). After granulation by granulating machine, compound filler was pressed into 2–4 cm, sprayed and cured for 5–7 days, until the strength was stable. Chemical compositions of three substrates were shown in Table 1. Three substrates were washed three times and air-dried.

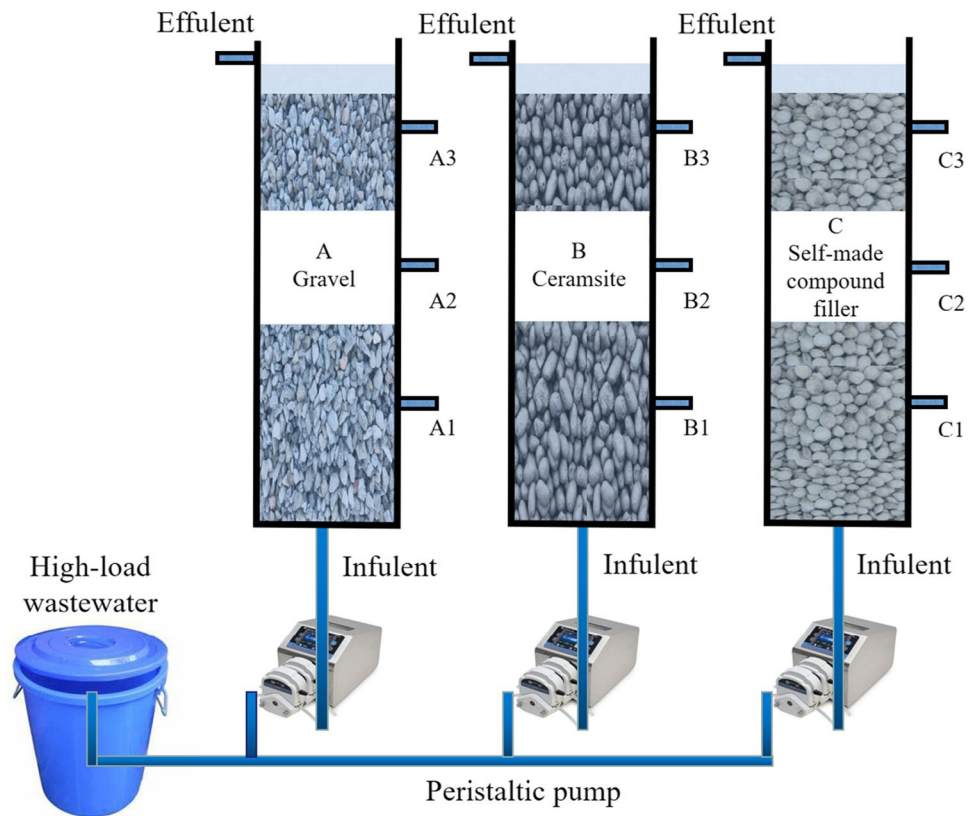
### Experimental setting of columns

Three laboratory-scale high-density polymethyl methacrylate columns with inner diameter of 10 cm and height of 80 cm were used as the experimental devices. The effective capacities of 3.8 L, 3.6 L and 3.53 L for the gravel, ceramsite and compound filler packed columns were measured, respectively. Three types of low-cost gravel ( $\Phi = 15\text{--}25$  mm), ceramsite ( $\Phi = 10\text{--}20$  mm) and self-made compound filler ( $\Phi = 20\text{--}25$  mm) were used as the main substrate layers in the columns with a height of ~63 cm, and the water outlet was set at a height of ~72 cm on the column. The experimental columns were placed indoors at Zhengzhou University, located in Zhengzhou, Henan, China. A schematic illustration of columns packed with three substrates was presented in Fig. 1. The seed sludge was obtained from the secondary sedimentation tank of Shuangqiao sewage treatment plant in Zhengzhou, Henan province, and inoculated two times

**Table 1** Chemical composition of three substrates (wt.%)

| Components                     | Gravel | Ceramsite | Compound filler<br>compound filler, |
|--------------------------------|--------|-----------|-------------------------------------|
| SiO <sub>2</sub>               | 11.47  | 25.46     | 29.198                              |
| Al <sub>2</sub> O <sub>3</sub> | 3.22   | 11.35     | 21.37                               |
| CaO                            | 8.12   | 1.25      | 28.54                               |
| Fe <sub>2</sub> O <sub>3</sub> | 4.02   | 5.99      | 6.17                                |
| MgO                            | 1.96   | 1.24      | 2.01                                |
| other                          | -      | -         | -                                   |

**Fig. 1** Schematic diagram of the experimental columns packed with different substrates (gravel, ceramsite and compound filler) under continuous operation



to promote biofilm formation. Relevant parameters of three columns were shown in Table A.1.

### Wastewater and experimental operation

In order to explore the purification ability of three kinds of substrates, a heavily polluted loads wastewater (eg. swine wastewater) in Henan province was taken as the research object to simulate the wastewater inflow. Synthetic high-load wastewater was used to better investigate the effect of substrates on the purification performance and microbial community of the three columns due to the minimal change in inlet water quality. The synthetic wastewater was composed of  $\text{CH}_3\text{COONa}$ : 0.8512 g/L,  $\text{NH}_4\text{Cl}$ : 0.133 g/L and  $\text{KH}_2\text{PO}_4$ : 0.0658 g/L and trace amounts of mineral solution (Chang et al. 2019). Tap water was used as raw material to simulate the high-load wastewater, containing  $\sim 325 \text{ mg}\cdot\text{L}^{-1}$  COD,  $\sim 35 \text{ mg}\cdot\text{L}^{-1}$   $\text{NH}_4^+\text{-N}$  and  $\sim 14 \text{ mg}\cdot\text{L}^{-1}$  TP. Wastewater was pumped into column through peristaltic pump (kamoer UIP, CK40200002) at speeds of 5.278 mL/min (A), 5 mL/min (B), and 4.903 mL/min (C) continuously. The hydraulic retention time was 8 h, and the hydraulic loading rates (HLR) were 968.146, 917.152 and 899.36  $\text{L}\cdot\text{m}^{-2}\cdot\text{d}^{-1}$ . The whole experiment operated at winter temperature and lasted from November 2021 to January 2022 with ambient temperature ranging from 0–15°C.

### Sampling and analysis

#### Substrates characterization and analysis

Three substrates were used to analyze the surface morphologies and elements constitute using scanning electron microscope (SEM) and energy dispersion spectrometry (EDS) (Helios G4 CX, Czech). The crystal structures and phase composition of substrates before and after experiment were analyzed via X-Ray Diffraction (D8 advance diffractometer, Bruker, German). The samples were scanned from 10° to 90°, and Jade 6.5 software was used to analyze the XRD patterns of the samples according to the standard PDF files (Li et al. 2021b).

#### Water sampling and analysis

The inlet and outlet water of three columns were collected each 2 days. Then the water samples were centrifuged for 10 min at 4000 r/min, and the supernatant was taken and further filtered with 0.45  $\mu\text{m}$  filter membrane for the analysis of chemical oxygen demand (COD), ammonia nitrogen ( $\text{NH}_4^+\text{-N}$ ), total nitrogen (TN) and total phosphorus (TP) according to the standard methods (Total et al. 1999). The pH values were measured with a pH meter (HI-2210, shanghai, China).

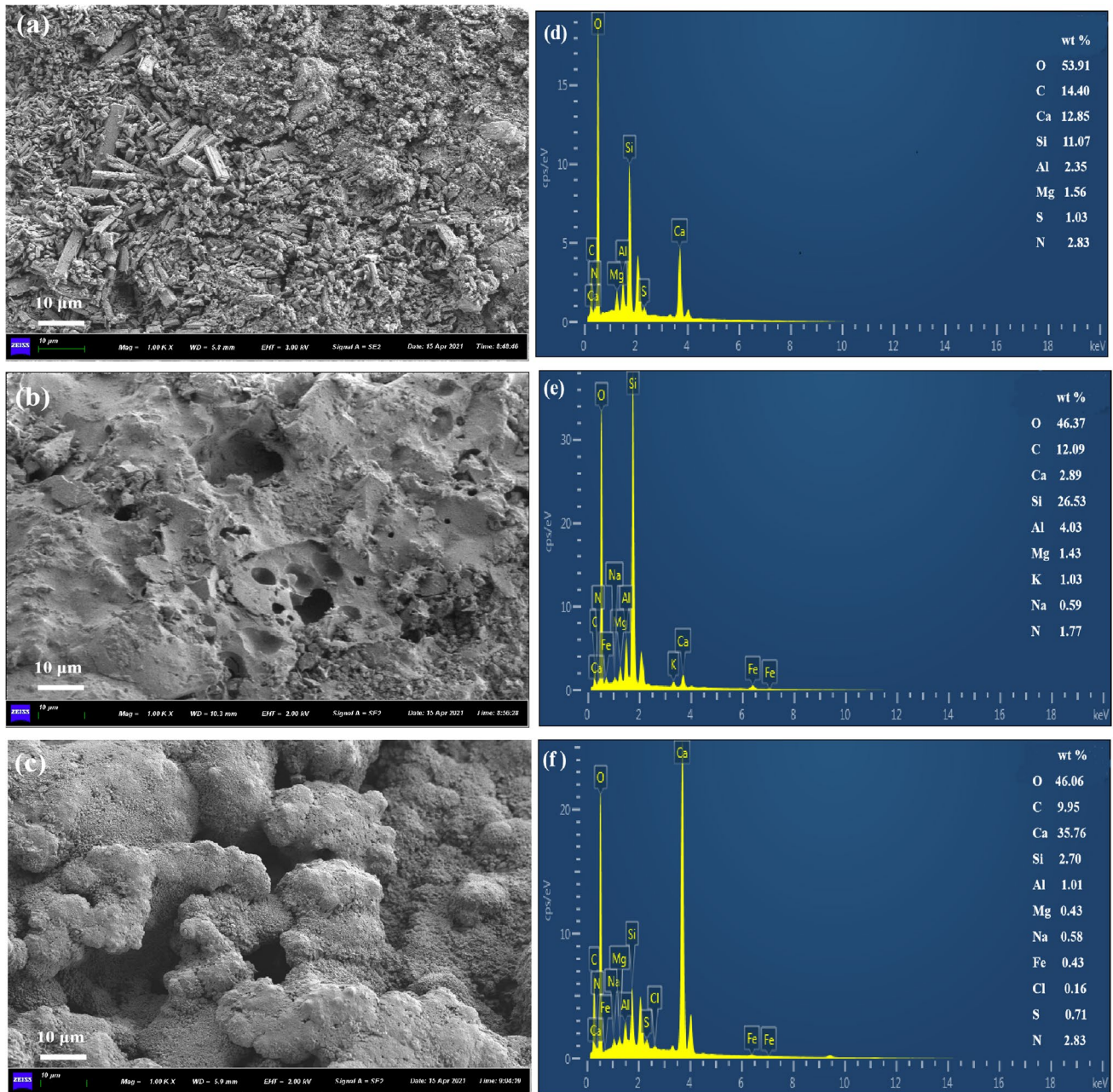


**Fig. 2** SEM observations on the surface of gravel (a), ceramsite (b), compound filler (c) and EDS spectrum on the surface of gravel (d), ceramsite (e), compound filler (f) before experiments

### Microorganism community analysis

After treatment, the substrates at the bottom, middle, and upper of columns were taken and mixed to explore the microbial community characteristics. The samples were stored in the refrigerator at  $-80^{\circ}\text{C}$  before being sent to Sangon Biotech (Shanghai, China) for high-throughput sequencing assay. DNA were extracted from biofilm of substrates and then amplified by PCR using the primers 338F (5'-ACTCCTACGGGAGGCAGCAG-3') and 805R

(5'-GACTACHVGGGTATCT AATCC-3'), and these targeted the V3–V4 regions of bacterial 16S rRNA genes (Liu et al. 2021).

### Experiments statistical analysis

SPSS 22.0 software (IBM, USA) was used to statistical analysis of the data. Analyses of STDEVA were used to evaluate the validity of the results. When the P value was lower than 0.05, the results were considered significant.

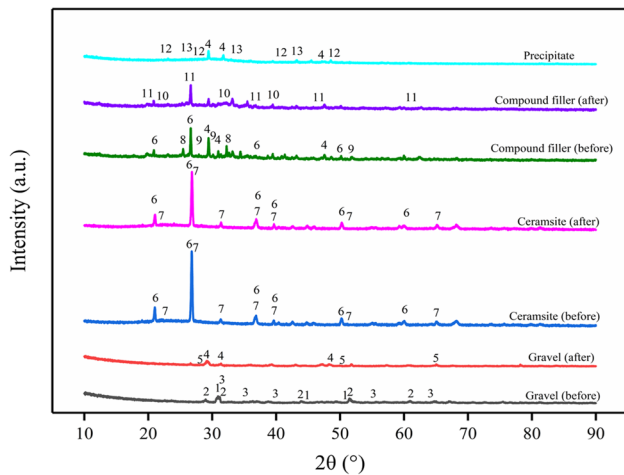


**Fig. 3** XRD patterns of the gravel, ceramsite and compound filler were analyzed before and after experiments

## Results and discussion

### Characterization of the substrates

#### SEM–EDS analyses

The SEM–EDS images of substrates were shown in Fig. 2. It was observed that the microstructure of compound filler was more obvious and the pores were larger than gravel and ceramsite. The surfaces of compound filler and ceramsite were rough, cracked and loose, while the surface of gravel was relatively dense and flat. The rough and loose surface is conducive to enhance adhere between the microbes and the substrates, and the numerous pores enlarge the specific surface area of the substrates, which is beneficial to the adsorption on the surface active sites (Liu et al. 2019). EDS images listed the element of substrate of three columns. The main components in compound filler were Ca (35.76%), Al (1.07%), Fe (0.43%) and Mg (0.43%), and the main elements of gravel were C (14.40%), Ca (12.85%), Al (2.35%) and Mg (1.56%), while the main elements of ceramsite were C (12.09%), Ca (2.89%), Al (4.03%) and Mg (1.43%). In general, Ca, Al, Fe and Mg were prone to hydrolyze and ligand exchange with phosphate in the process of wastewater purification, this was the reason that the phosphorus removal effect of the compound filler was better than that of gravel and ceramsite.

#### Mineralogical phase analysis

The XRD patterns of the substrates before and after the test were presented in Fig. 3. The characteristic diffraction peaks at different  $2\theta$  (°) were analyzed with Jade 6.5, and the results showed that the main compositions of the gravel

before the reaction were ankerite:  $\text{Ca}(\text{Fe}\cdot 2\text{Mg})(\text{CO}_3)_2$  (1), gypsum:  $\text{CaSO}_4\cdot 2\text{H}_2\text{O}$  (2), calcium zinc aluminum oxide:  $\text{Ca}_3\text{Al}_4\text{ZnO}_{10}$  (3), the main components of the ceramsite before the reaction were quartz:  $\text{SiO}_2$  (6), gismondine:  $\text{CaAl}_2\text{Si}_2\text{O}_8\cdot 4\text{H}_2\text{O}$  (7), and the main compositions of the compound filler before reaction were calcite:  $\text{CaCO}_3$  (4), quartz:  $\text{SiO}_2$  (6), calcium aluminum oxide  $\text{CaAl}_4\text{O}_4$  (8), dellaite:  $\text{Ca}_5(\text{SiO}_4)_2(\text{OH})_2$  (9). Calcium, aluminum and iron compounds have excellent potential in phosphorus removal, that have also been reported in previous studies (Li et al. 2021b; Cheng et al. 2018). At the end of the column test running, the characterization of the substrates was found that the main compositions of the gravel were calcite:  $\text{CaCO}_3$  (4); xonotlite  $\text{Ca}_6\text{Si}_6\text{O}_{17}(\text{OH})_2$  (5); the components of the ceramsite were not changed, which was as follows: quartz:  $\text{SiO}_2$  (6); gismondine:  $\text{CaAl}_2\text{Si}_2\text{O}_8\cdot 4\text{H}_2\text{O}$  (7); and the main components of the compound filler were aluminium hydroxide sulfate:  $\text{AlSO}_4(\text{OH})\cdot 5\text{H}_2\text{O}$  (10), calcium phosphate silicate:  $\text{Ca}_2\text{SiO}_4\cdot 0.05\text{Ca}_3(\text{PO}_4)_2$  (11). It was observed that the crystallization peaks of calcium, iron and aluminum were weakened to some extent, indicating that these elements played an important role in phosphate removal. Besides, abundant white precipitates could be clearly identified on the C-column during the initial operation period (Fig. A.1), which was identified as calcite:  $\text{CaCO}_3$  (4), dellaite  $\text{Ca}_6(\text{SiO}_4)(\text{Si}_2\text{O}_7)(\text{OH})_2$  (12), calcium silicate hydroxide  $(\text{Ca}_7\text{Si}_{16}\text{O}_{38}(\text{OH})_2$  (13) by Jade 6.5 analysis. This white precipitates confirmed that the formation of  $\text{CaCO}_3$  crystals in the C-column was the result of  $\text{CO}_2$  diffusion and alkalinity by metal ions hydrolyzed, and enhanced the possibility of co-precipitation of  $\text{CaCO}_3$  on calcium phosphates (Blanco et al. 2016). Besides, calcite provides sorption sites for phosphate, resulting in the nucleation, and precipitation of calcium phosphates has also been reflected in relevant literature (Liira et al. 2009; Blanco et al. 2016).

### Pollutant purification performance of columns

#### Organic matter removal

The removal rates and concentrations of  $\text{COD}_{\text{cr}}$  in inlet and outlet water of three columns packed self-made compound filler, gravel, and ceramsite substrates were compared. As shown in Fig. 4(a) and (b), the removal of  $\text{COD}_{\text{cr}}$  (A:21%–65%, B:18%–59%, C:11–55%) were different slightly despite the high concentration (~300 mg/L), regardless of the packed different substrates in columns. Two phases of the experiment could be distinguished a starting phase and stable phase, during the starting period, the removal efficiency of  $\text{COD}_{\text{cr}}$  increased from 21 to 51%, 18% to 42% and 11% to 35% with effluent concentrations changed from 249 mg/L to 149 mg/L, 256 mg/L to 177 mg/L and 279 mg/L

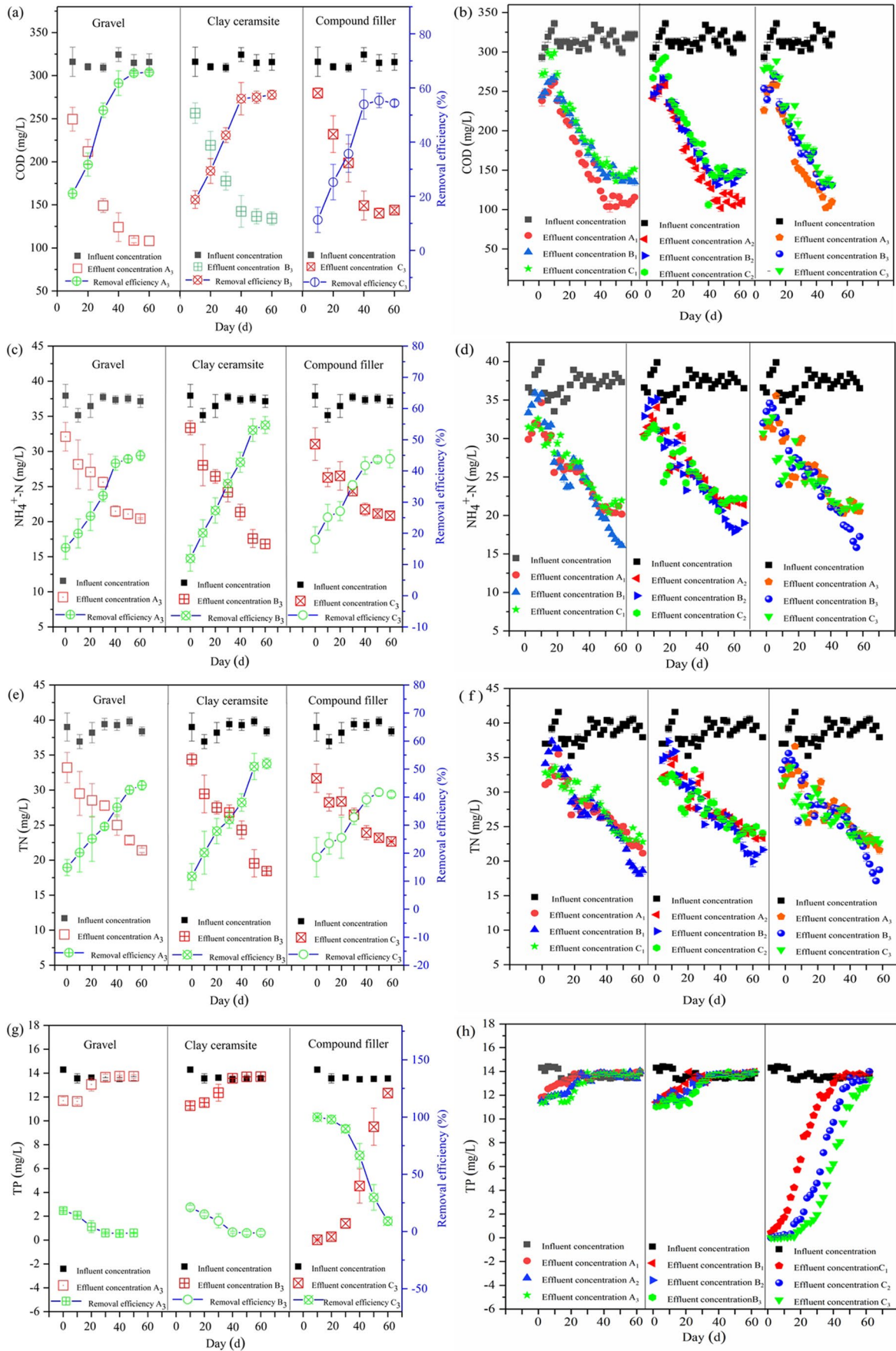


**Fig. 4** Average removal efficiencies, influent and effluent concentrations of COD (a) and (b),  $\text{NH}_4^+\text{-N}$  (c) and (d), TN (e) and (f), TP (g) and (h) in columns packed with different substrates (gravel, ceramsite and self-made compound filler) under continuous flow trials at the hydraulic retention time of 8 h (HRT: 8 h)

to 198 mg/L in A-column, B-column and C-column, respectively. During the stable period, the average  $\text{COD}_{\text{cr}}$  removal efficiencies were 64%, 56% and 54% in A-column, B-column and C-column, respectively. The average effluent concentration of  $\text{COD}_{\text{cr}}$  in A-column was 113 mg/L, which was lower than those of B-column (137 mg/L) and C-column (144 mg/L). The results showed that A-column had slightly more removal efficiency of  $\text{COD}_{\text{cr}}$  than B-column and C-column, even if the difference was not significant.

The removal of organics matter are results of adsorption by substrates and assimilation by microorganisms with the increased biomass, and the substrate with larger specific surface area and more micropores has better effect on removal of pollutants in CWs (Tan et al. 2019). Combining with the two period of organic removal, it can be seen that the removal of organic mainly depends on microbial enrichment and assimilation.

### Nitrogen removal

Figure 4(c) and (d) showed the average removal efficiencies and the concentrations of  $\text{NH}_4^+\text{-N}$  in inlet and outlet water in three columns with different substrates. It was found that the effluent of  $\text{NH}_4^+\text{-N}$  concentrations decreased gradually with the running to 40 d, and then an average  $\text{NH}_4^+\text{-N}$  effluent concentrations of 21.48 mg/L and removal efficiency of 42.46% was reached in A-column, while in B-column and C-column these values were 21.35 mg/L and 42.78%, 21.75 mg/L and 41.73%, respectively. During the starting time, the main removal mechanism of  $\text{NH}_4^+\text{-N}$  might be the absorption of substrates, while in the stable time,  $\text{NH}_4^+\text{-N}$  removal might be dominated by microorganisms nitrification (Wang et al. 2020; Li et al. 2021a, b).

The removal of TN was also measured, and it was found to be a stable period after 40 days (Fig. 4(e) and (f)), which was consistent with the removal of  $\text{NH}_4^+\text{-N}$ . During the starting period, the removal efficiency of TN increased from 14 to 36%, 11% to 40% and 18% to 39% with effluent concentrations changed from 33 mg/L to 25 mg/L, 34 mg/L to 24 mg/L and 31 mg/L to 23 mg/L in A-column, B-column and C-column, respectively. Moreover, in the stable period, the average removal efficiencies were 41.67% for A-column, 46.95% for B-column, 40% for C-column, respectively. There were no significant differences between three columns, indicating that the different packed substrates did not have significant effects on TN removal. As reported,

the removal of nitrogen in CWs is a comprehensive process involving biological and physicochemical effects, which is realized by ammoniation, nitrification, denitrification and plant uptake (Gao et al. 2018; Li et al. 2021a). The TN removal rates of three columns increased before 40 days, which was mainly depended on the adsorption of substrates, and the nitrification and denitrification of the microorganisms accounted for a small part (Liu et al. 2020). The TN removal rates of the three columns were stable, and might be attributed to the assimilation, nitrification and denitrification of the microorganisms while the adsorption of substrates played a minor role.

In general, the removal rate for nitrogen in each column was not ideal. The lower nitrogen removal rate of three columns might be related to the low temperature (0–15°C). The decreased activity of denitrifying microorganisms might be limited nitrogen removal process below 15°C (Kumar and Lin 2010; Li et al. 2021a).

### Phosphorus removal

As shown in Fig. 4(g) and (h), a significant difference in TP removal efficiencies were observed among three columns with 0–18% in A-column, 0–21% in B-column and 9%–99% in C-column. The effluent TP concentrations increased from 11.7 mg/L to 13.9 mg/L, 11.2 mg/L to 13.9 mg/L and 0.017 mg/L to 13.3 mg/L in A-column, B-column and C-column, respectively. These results suggested that compound filler was a promising novel substrates and can effectively remove phosphorus from wastewater, These was mainly attributed to the compound filler rich in Al, Ca, Mg and Fe and  $\text{PO}_4^{3-}$  could be removed by  $\text{Ca}^{2+}$ ,  $\text{Al}^{3+}$ ,  $\text{Fe}^{3+}$  and other ions to form insoluble compounds in interstitial water or by ligand exchanging with hydrated metal ions on the surface of substrate and incorporated into its crystal lattice, which had been reflected in relevant studies (Yang et al. 2018; Li et al. 2021b; Cerozi and Fitzsimmons 2016; Li et al. 2021a).

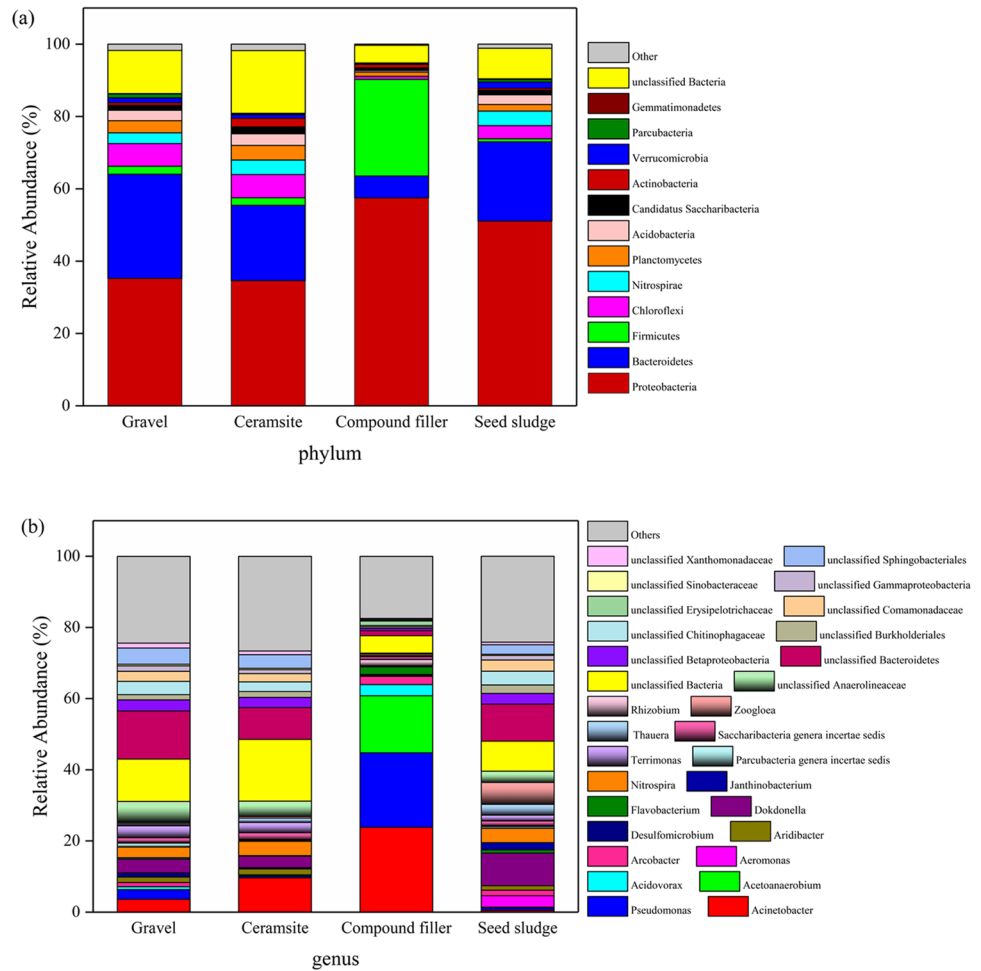
### Kinetic modelling of three columns in phosphorus removal

In order to evaluate the phosphate removal performance of gravel/ceramsite/compound filler, the breakthrough curves of three columns were plotted using  $C_t/C_0$  ratios (outlet to inlet phosphorus concentration). The TP adsorbed in the column ( $q_{\text{total}}$ ) and exhausted time ( $t_e$ ) can be calculated from the area under the breakthrough curve (Rout et al. 2017). The breakthrough curves of three columns at different depths of 20 cm, 40 cm and 60 cm with the same flow rate and influent phosphorus concentration were given in Fig. A.2. It can be seen from the results that an increase in depths from 20 to 40 to 60 cm led to an increase in exhaustion times from 11 to 15 to 21 d of A-column, 13 to 19 to 27 d of B-column and 37 to 45

**Table 2** Microbial diversity and richness of biofilm in three columns packed with different substrates (gravel, ceramsite, compound filler)

| Sample          | Number | OTUs | Shannon | Chao    | ACE     | Simpson | Shannon | Coverage |
|-----------------|--------|------|---------|---------|---------|---------|---------|----------|
| Gravel          | 55,185 | 1169 | 5.51    | 1219.79 | 1200.72 | 0.01    | 0.78    | 1.00     |
| Ceramsite       | 50,808 | 1136 | 5.35    | 1190.85 | 1174.83 | 0.02    | 0.76    | 1.00     |
| Compound filler | 57,020 | 893  | 3.44    | 1068.51 | 1032.65 | 0.09    | 0.51    | 1.00     |
| Seed sludge     | 57,791 | 1082 | 5.10    | 1140.70 | 1134.43 | 0.02    | 0.73    | 1.00     |

**Fig. 5** Bacterial community composition at the phylum (a) and genus (b) levels of substrates and seed sludge. Phyla and genera making up less than 1% of the compositions are defined as others



to 55 d of C-column, respectively. Breakthrough volume and exhaustion also increased with depths. In addition, the slope of the breakthrough curves became flatter as the increasing column depths, resulting in the expansion of the mass transfer zone, similar results have been found in previous studies (Cusack et al. 2019; Rout et al. 2017). This phenomenon may be due to the longer contact time of empty bed with the increase of column depths, which further improved the contact time between phosphate and substrates. Moreover, as the depth of the column

increases, more adsorbents can be accommodated, more adsorbent surface area and phosphate-binding active sites were provided.

To further analyze the dynamic adsorption behavior of phosphorus on the columns, Thomas and Yoon-Nelson model were adopted to fit the experiment data. Apart from providing a more accurate description of the penetration curves, these models are useful in providing valuable system parameters for the adsorption processes in engineering-scale CWs.



Thomas model assumes that the adsorption process follows the second-order reaction kinetics and Langmuir isotherm, and no axial dispersion (Chu 2020; Rout et al. 2017). The simplified linear form of Thomas model is as follows:

$$\ln \left[ \frac{C_0}{C_t} - 1 \right] = \frac{k_{Th}mq_e}{Q} - k_{Th}C_0t \quad (1)$$

where  $C_t$  is the outlet concentration (mg/L),  $C_0$  is the inlet concentration (mg/L),  $k_{Th}$  is Thomas's rate constant (mL/(mg·d)),  $m$  is the mass of adsorbent (g),  $q_e$  is the adsorption capacity at the equilibrium (P g/kg),  $Q$  is flow rate (mg/min),  $t$  is flow time (d).

The simplified linear form of Yoon-Nelson model is as follows:

$$\ln \left[ \frac{C_t}{C_0 - C_t} \right] = k_{YN}t - t_{1/2}k_{YN} \quad (2)$$

where  $C_t$  is the outlet concentration (mg/L),  $C_0$  is the inlet concentration (mg/L),  $k_{YN}$  is Yoon-Nelson's rate constant (1/d),  $t_{1/2}$  is the breakthrough time for 50% adsorbent (g),  $t$  is flow time (d).

The phosphate adsorption data were fitted to the Thomas model and Yoon-Nelson model by linear regression method, and the prediction experimental curves were shown in Fig. A.3, the related model parameters were listed in Table A.2. As listed in Table A.2, the Thomas model fitting constant  $R^2$  of compound filler (0.932) is significantly better than that of Gravel (0.836) and Ceramsite (0.717). Besides, the Yoon-Nelson model also showed the similar results, which indicated that phosphorus removal mainly occurred by adsorption in the compound fillers during operation of column, while gravel and ceramsite may have other functions besides adsorption (i. e. microbial). The maximum adsorption capacity of compound filler (683 P g/kg) was larger than those of gravel (213 P g/kg) and ceramsite (468 P g/kg), and breakthrough time was significantly longer than gravel and ceramsite.

### Microbial community in three substrates analysis

The microbial communities in columns packed with three substrates were investigated by high-throughput sequencing for 16S rRNA genes. The effective sequences, taxonomic OTUs and bacterial diversity estimation richness (Chao1 and ACE) and indicators (Simpson and Shannon) of biofilm on the substrates in columns are listed in Table 2. The rarefaction curves of Alpha index reached plateau (Fig.A.4), indicating that the sequencing depths were close to the actual microbial community characteristics (Jena et al. 2016). The

Venn diagram (Fig. A.5) showed that more than 751 OTUs were shared among three substrates and seed sludge, while the numbers of OTUs unique of gravel (A-column), ceramsite (B-column), compound filler (C-column) and seed sludge were 8 (0.68%), 3 (0.26%), 3 (0.34%) and 15 (1.39%), respectively, indicating that no significant distinct bacterial communities were formed on the substrates. The Shannon index and Chao value indicated that compound filler was not favorable for the microbial diversity and richness compared with gravel and ceramsite in general, which may be because the alkaline pH (7.8–8.9) caused by compound filler was not conducive to the growth of bacteria (Xiao et al. 2020; Chang et al. 2019). This result also explained why the compound filler worked lower than gravel and ceramsite in the purification of pollutants such as COD,  $\text{NH}_4^+\text{-N}$  and TN.

A total of 12 dominant bacterial phyla were detected in three substrates and seed sludge, and phyla with less than 1% composition were defined as other (Fig. 5(a)). There were significant differences in the compositions of bacterial communities in three columns, indicating that the column substrates with different properties formed bacterial communities after inoculation with the same seed sludge (Zhao et al. 2017; Chang et al. 2019). The phylum of *Proteobacteria* was predominant in all samples, accounting for 57.48% of the total bacteria in column-compound filler, while others only occupied 35.20%, 34.60%, 51.09% in column-gravel, column-ceramsite and seed sludge, respectively. The results showed that the compound filler had a good affinity for *Proteobacteria*. *Proteobacteria* is known to be important in wastewater purification because it contains a variety of bacteria involved in carbon, nitrogen and sulfur cycling, and has been reported in other studies of wetlands (Ge et al. 2019; Pishgar et al. 2019; Liu et al. 2020). Followed by phylum *Firmicutes*, *Bacteroidetes*, *Planctomycetes*, with the proportion of 26.75%, 6.06% and 1.18% in column-compound filler, respectively, the relative abundance of other phyla was less than 1%. Compared with C-column-compound filler, the phyla of *Firmicutes*, *Bacteroidetes*, *Chloroflexi*, *Planctomycetes*, *Nitrospirae* and *Acidobacteria* were also dominant, accounting for 2.19%, 28.86%, 6.27%, 3.38%, 2.97% and 2.86% in column-gravel (A), 2.08%, 20.85%, 6.43%, 4.05%, 4% and 3.21% in column-ceramsite (B), 0.86%, 21.91%, 3.62%, 1.82%, 4.04% and 2.65% in seed sludge, respectively. *Bacteroidetes* is a group with a variety of chemoheterotrophic genera bacteria, which has strong ability to degrade organic pollutants, is also dominant (20.82%–28.86%) in column-gravel (A) and column-ceramsite (B), probably as the reason for the lower concentration of COD in effluent water (Silveira et al. 2021; Deng et al. 2021).

The main genera with relative abundances above 1% in substrates and seed sludge were shown in Fig. 5(b). A total of 30 genera were detected from all substrates, with

fewer in compound filler compared to other substrates, which was consistent with the lower Shannon index (3.44) and phylum level (5) of this sample. In column-compound filler (C), only *Acinetobacter* (23.84% of the total sequences), *Pseudomonas* (20.93%), *Acetoanaerobium* (16.05%), *Acidovorax* (3.12%), *Arcobacter* (2.31%), *Flavobacterium* (2.12%) were the dominant species in the bacterial community, while the content of these genera was relatively lower in other substrates. These results indicated that the compound filler was more conducive as a supporter to the growth of *Pseudomonas* and *Acetoanaerobium* than gravel and ceramsite. The genus *Pseudomonas* belongs to *Proteobacteria*, improves the ability of phosphorus removal and denitrification (Kong et al. 2017; Xiao et al. 2020). *Acinetobacter*, *Acetoanaerobium* and *Acidovorax* were reported to be aerobic heterotrophic bacteria capable of ammonium oxidation, nitrification and denitrification (Xia et al. 2020; Pang et al. 2020; Fu and Zhao 2015), indicating that the compound filler may have an excellent potential for  $\text{NH}_4^+$ -N,  $\text{NO}_3^-$ -N and TN removal in the subsequent purification process. Overall, although the addition of compound filler reduced the abundance of bacterial communities than other substrates, it promoted the enrichment of functional bacteria that were conducive to nitrogen and organic contaminant degradation. The abundance of heat map was consistent with this conclusion (Fig. A.6).

## Conclusion

The results of this study indicated that the self-made compound filler was a potential substrate for CWs. Under the high-phosphorus load wastewater and low-temperature conditions, the phosphorus removal efficiency of compound filler (9–99%) was better than those of gravel (0–18%) and ceramsite (0–21%). The average removal efficiencies of COD,  $\text{NH}_4^+$ -N and TN of compound filler were slightly lower than those of gravel and ceramsite, which was related to the inhibition of some microbial activities by compound filler. However, the proportion of aerobic heterotrophic bacteria (i.e. *Pseudomonas*, *Acinetobacter*, and *Acetoanaerobium*) with ammonium oxidation, nitrification and denitrification was enhanced by the compound filler.

**Supplementary Information** The online version contains supplementary material available at <https://doi.org/10.1007/s11356-023-26487-3>.

**Acknowledgements** Thanks to Professor Zhao Yaqian of Xi'an University of Technology/University of Dublin for his theoretical guidance. Thanks to the Graduate Independent Innovation Fund of Zhengzhou University. This research was supported by the National Science and Technology Major Project (2017ZX07602-003-002) and by the Major Special Science and Technology Project

of Henan Province (181100310300), the Research Fund of Key Laboratory of Water Management and Water Security for Yellow River Basin, Ministry of Water Resources (under construction) (2022-SYSJJ-XX), ZHONGYUAN YINGCAI JIHUA (ZYYCYU202012183), the Henan Key Scientific Research Projects (23B610004), the fellowship of China Postdoctoral Science Foundation (2020TQ0284 and 2020M682355), the Henan Postdoctoral Foundation (202003027), and the Opening Project of Henan Province Key Laboratory of Water Pollution Control and Rehabilitation Technology (CJSP2021007).

**Authors contributions** Qiang Li: Conceptualization, Formal analysis, Data Curation, Visualization, Writing—Original Draft, Writing—Review & editing.

Jingqing Gao: Conceptualization, Supervision, Resources, Funding acquisition, Project administration, Writing—review & editing, Validation.

Jingshen Zhang: Formal analysis, Resources, Supervision, Methodology, Validation.

Zhenzhen Huang: Investigation, Writing—review & editing, Project administration, Supervision, Validation.

Shilong Wang: Investigation, Software.

Bozhen Song: Supervision, Writing—Review & editing.

Qiaojian Wang: Investigation, Methodology.

Wanglin Zhou: Resources.

**Funding** National Science and Technology Major Project (2017ZX07602-003-002),

Major Special Science and Technology Project of Henan Province (181,100,310,300),

The fellowship of China Postdoctoral Science Foundation (2020TQ0284 and 2020M682355),

The Research Fund of Key Laboratory of Water Management and Water Security for Yellow River Basin, Ministry of Water Resources (under construction) (2022-SYSJJ-XX),

ZHONGYUAN YINGCAI JIHUA (ZYYCYU202012183),

Henan Key Scientific Research Projects (23B610004),

Henan Postdoctoral Foundation (202,003,027),

The Opening Project of Henan Province Key Laboratory of Water Pollution Control and Rehabilitation Technology (CJSP2021007).

**Data availability** The datasets used and/or analysed during the current study are available from the corresponding author on reasonable request.

## Declarations

**Ethical Approval** Not applicable.

**Consent to Participate** Not applicable.

**Consent to Publish** Not applicable.

**Competing Interests** The authors declare that they have no competing interests.

## References

- Blanco I, Molle P, Sáenz de Miera LE, Ansola G (2016) Basic Oxygen Furnace steel slag aggregates for phosphorus treatment: evaluation of its potential use as a substrate in constructed wetlands. *Water Res* 89:355–365. <https://doi.org/10.1016/j.watres.2015.11.064>

- Brix H, Arias CA, Del Bubba M (2001) Media selection for sustainable phosphorus removal in subsurface flow constructed wetlands. *Water Sci Technol* 44:47–54. <https://doi.org/10.2166/wst.2001.0808>
- Cerozi S, Fitzsimmons K (2016) The effect of pH on phosphorus availability and speciation in an aquaponics nutrient solution. *Bioresour Technol* 8–11. <https://doi.org/10.1016/j.biortech.2016.08.079>
- Chang J, Mei J, Jia W, Chen J, Li X, Ji B, Wu H (2019) Treatment of heavily polluted river water by tidal-operated biofilters with organic/inorganic media: evaluation of performance and bacterial community. *Bioresour Technol* 279:34–42. <https://doi.org/10.1016/j.biortech.2019.01.060>
- Cheng G, Li Q, Su Z, Sheng S, Fu J (2018) Preparation, optimization, and application of sustainable ceramsite substrate from coal fly ash/waterworks sludge/oyster shell for phosphorus immobilization in constructed wetlands. *J Clean Prod* 175:572–581. <https://doi.org/10.1016/j.jclepro.2017.12.102>
- Chu KH (2020) Breakthrough curve analysis by simplistic models of fixed bed adsorption : in defense of the century-old Bohart-Adams model. *Chem Eng J* 380:122513. <https://doi.org/10.1016/j.cej.2019.122513>
- Cusack PB, Callery O, Courtney R, Ujaczki É, O'Donoghue LMT, Healy MG (2019) The use of rapid, small-scale column tests to determine the efficiency of bauxite residue as a low-cost adsorbent in the removal of dissolved reactive phosphorus from agricultural waters. *J Environ Manage* 241:273–283. <https://doi.org/10.1016/j.jenvman.2019.04.042>
- Deng H, Fu Q, Li D, Zhang Y, He J, Feng D, Zhao Y, Du G, Yu H, Ge C (2021) Microplastic-associated biofilm in an intensive mariculture pond: temporal dynamics of microbial communities, extracellular polymeric substances and impacts on microplastics properties. *J Clean Prod* 319:128774. <https://doi.org/10.1016/j.jclepro.2021.128774>
- Fu Z, Zhao J (2015) Impact of quinoline on activity and microbial culture of partial nitrification process. *Bioresour Technol* 197:113–119. <https://doi.org/10.1016/j.biortech.2015.08.067>
- Gao JQ, Zhao J, Zhang JS, Li Q, Gao JL, Cai M, Zhang JL (2020) Preparation of a new low-cost substrate prepared from drinking water treatment sludge (DWTS)/bentonite/zeolite/fly ash for rapid phosphorus removal in constructed wetlands. *J Clean Prod* 261:121110. <https://doi.org/10.1016/j.jclepro.2020.121110>
- Gao Y, Zhang W, Gao B, Jia W, Miao A, Xiao L, Yang L (2018) Highly efficient removal of nitrogen and phosphorus in an electrolysis-integrated horizontal subsurface-flow constructed wetland amended with biochar. *Water Res* 139:301–310. <https://doi.org/10.1016/j.watres.2018.04.007>
- Ge Z, Wei D, Zhang J, Hu J, Liu Z, Li R (2019) Natural pyrite to enhance simultaneous long-term nitrogen and phosphorus removal in constructed wetland: three years of pilot study. *Water Res* 148:153–161. <https://doi.org/10.1016/j.watres.2018.10.037>
- Habibiandehkordi R, Quinton JN, Surridge BWJ (2014) Effect of equilibration time on estimates of the maximum phosphorus sorption capacity of industrial by-products using the Langmuir model. *J Soils Sediments* 14:1818–1828. <https://doi.org/10.1007/s11368-014-0936-y>
- Jena J, Kumar R, Dixit A, Das T (2016) Anoxic-aerobic SBR system for nitrate, phosphate and COD removal from high-strength wastewater and diversity study of microbial communities. *Biochem Eng J* 105:80–89. <https://doi.org/10.1016/j.bej.2015.09.007>
- Kong Q, He X, Feng Y, Miao M, Wang Q, Du Y, Xu F (2017) Pollutant and microorganism evolution of activated sludge under ofloxacin selection pressure. *Bioresour Technol* 241:849–856. <https://doi.org/10.1016/j.biortech.2017.06.019>
- Kumar M, Lin J (2010) Co-existence of anammox and denitrification for simultaneous nitrogen and carbon removal — strategies and issues. *J Hazard Mater* 178:1–9. <https://doi.org/10.1016/j.jhazmat.2010.01.077>
- Li H, Zhang Y, Wu L, Jin Y, Gong Y, Li A, Li J (2021) Recycled aggregates from construction and demolition waste as wetland substrates for pollutant removal. *J Clean. Prod.* 311:127766. <https://doi.org/10.1016/j.jclepro.2021.127766>
- Li Q, Zhang J, Gao J, Huang Z, Zhou H, Duan H, Zhang Z (2021b) Preparation of a novel non-burning polyaluminum chloride residue(PACR) compound filler and its phosphate removal mechanisms. *Environ Sci Pollut Res.* <https://doi.org/10.1007/s11356-021-15724-2>
- Liira M, Kõiv M, Mander Ü, Mõtlep R, Vohla C, Kirsimäe K (2009) Active filtration of phosphorus on ca-rich hydrated oil shale ash: does longer retention time improve the process? *Environ Sci Technol* 43:3809–3814. <https://doi.org/10.1021/es803642m>
- Liu C, Li X, Yang Y, Fan X, Tan X, Yin W, Liu Y, Zhou Z (2020) Double-layer substrate of shale ceramsite and active alumina tidal flow constructed wetland enhanced nitrogen removal from decentralized domestic sewage. *Sci Total Environ* 703:135629. <https://doi.org/10.1016/j.scitotenv.2019.135629>
- Liu Ff, Fan J, Du J, Shi X, Zhang J, Shen Y (2019) Intensified nitrogen transformation in intermittently aerated constructed wetlands: removal pathways and microbial response mechanism. *Sci Total Environ* 650:2880–2887. <https://doi.org/10.1016/j.scitotenv.2018.10.037>
- Liu L, Li N, Tao C, Zhao Y, Gao J (2021) Nitrogen removal performance and bacterial communities in zeolite trickling filter under different influent C / N ratios. *Env Sci Pollut Res* 28:15909–15922. <https://doi.org/10.1007/s11356-020-11776-y>
- Lu D, Qi Z, Li M, Zhang Y, Chen Y, Qi Y, Wu H (2021) Organics and nutrient removal from swine wastewater by constructed wetlands using ceramsite and magnetite as substrates. *J Environ Chem Eng* 9:104739. <https://doi.org/10.1016/j.jece.2020.104739>
- Pang L, He Y, Liu X, Li J, Yang P (2020) The role of a newly isolated strain *Corynebacterium pollutisoli* SPH6 in waste activated sludge alkaline fermentation. *Chemosphere* 241. <https://doi.org/10.1016/j.chemosphere.2019.125072>
- Pishgar R, Dominic JA, Sheng Z, Tay JH (2019) Denitrification performance and microbial versatility in response to different selection pressures. *Bioresour Technol* 281:72–83. <https://doi.org/10.1016/j.biortech.2019.02.061>
- Rout PR, Bhunia P, Dash RR (2017) Evaluation of kinetic and statistical models for predicting breakthrough curves of phosphate removal using dolochar-packed columns. *J Water Process Eng* 17:168–180. <https://doi.org/10.1016/j.jwpe.2017.04.003>
- Scholes L, Faulkner H, Tapsell S, Downward S (2008) Urban rivers as pollutant sinks and sources: A public health concern for recreational river users? *Water Air Soil Pollut Focus* 8:543–553. <https://doi.org/10.1007/s11267-008-9178-6>
- Sheng Y, Qu Y, Ding C, Sun Q, Mortimer RJG (2013) A combined application of different engineering and biological techniques to remediate a heavily polluted river. *Ecol Eng* 57:1–7. <https://doi.org/10.1016/j.ecoleng.2013.04.004>
- Silveira NC, Oliveira GHD, Damianovic MHRZ, Foresti E (2021) Two-stage partial nitrification-Anammox process for nitrogen removal from slaughterhouse wastewater: Evaluation of the nitrogen loading rate and microbial community analysis. *J Environ Manage* 296:113214. <https://doi.org/10.1016/j.jenvman.2021.113214>
- Tan X, Yang Y, Liu Y, Li X, Fan X, Zhou Z, Liu C, Yin W (2019) Enhanced simultaneous organics and nutrients removal in tidal flow constructed wetland using activated alumina as substrate treating domestic wastewater. *Bioresour Technol* 280:441–446. <https://doi.org/10.1016/j.biortech.2019.02.036>
- Total, S., Membrane, C., Procedure, F., 1999. Standard Methods for the Examination of Water and Wastewater Standard Methods for the Examination of Water and Wastewater.

- Wang, H., Xu, J., Sheng, L., 2020. Purification mechanism of sewage from constructed wetlands with zeolite substrates : A review. *J. Clean. Prod.* 258, 120760. <https://doi.org/10.1016/j.jclepro.2020.120760>
- Wang Z, He S, Huang J, Zhou W, Chen W (2018) Comparison of heterotrophic and autotrophic denitrification processes for nitrate removal from phosphorus-limited surface water. *Environ Pollut* 238:562–572. <https://doi.org/10.1016/j.envpol.2018.03.080>
- Wu H, Zhang J, Ngo HH, Guo W, Hu Z, Liang S, Fan J, Liu H (2015) A review on the sustainability of constructed wetlands for wastewater treatment: Design and operation. *Bioresour Technol* 175:594–601. <https://doi.org/10.1016/j.biortech.2014.10.068>
- Xia, L., Li, X., Fan, W., Wang, J., 2020. Heterotrophic nitrification and aerobic denitrification by a novel *Acinetobacter* sp . ND7 isolated from municipal activated sludge. *Bioresour. Technol.* 301, 122749. <https://doi.org/10.1016/j.biortech.2020.122749>
- Xiao, J., Huang, J., Huang, M., Chen, M., Wang, M., 2020. Application of basalt fiber in vertical flow constructed wetland for different pollution loads wastewater: Performance, substrate enzyme activity and microorganism community. *Bioresour. Technol.* 318, 124229. <https://doi.org/10.1016/j.biortech.2020.124229>
- Yang Y, Zhao Y, Liu R, Morgan D (2018) Global development of various emerged substrates utilized in constructed wetlands. *Bioresour Technol* 261:441–452. <https://doi.org/10.1016/j.biortech.2018.03.085>
- Zhao J, Feng L, Yang G, Dai J, Mu J (2017) Development of simultaneous nitrification-denitrification ( SND ) in biofilm reactors with partially coupled a novel biodegradable carrier for nitrogen-rich water purification. *Bioresour Technol* 243:800–809. <https://doi.org/10.1016/j.biortech.2017.06.127>

**Publisher's note** Springer Nature remains neutral with regard to jurisdictional claims in published maps and institutional affiliations.

Springer Nature or its licensor (e.g. a society or other partner) holds exclusive rights to this article under a publishing agreement with the author(s) or other rightsholder(s); author self-archiving of the accepted manuscript version of this article is solely governed by the terms of such publishing agreement and applicable law.